



# Assessing the Effect of Seawater and Magnesium Sulfate on the Durability and Strength Properties of Cement-Stabilized Full-Scale Soilcrete Column Constructed in Clayey Soil

Mustafa F. Hasan<sup>1</sup> · Hanifi Canakci<sup>2</sup>

Received: 30 November 2021 / Accepted: 20 February 2022  
© King Fahd University of Petroleum & Minerals 2022

## Abstract

Jet grouting techniques have lately become one of the soil enhancement technologies used to increase the strength of poor soils and resolve most of their difficulties. Seven full-scale soilcrete columns (SC) were formed in clayey soil using a one-to-one water-to-cement ratio and different parameters, including five different pressures (30, 32.5, 35, 37.5, and 40 MPa) and three different rotating rates (25, 35, 45 rpm). These metrics were used to assess SC's resistance to chemical attacks [seawater, magnesium sulfate ( $\text{MgSO}_4$ )]. Additionally, it is also working on the strength investigation (unconfined compression test) of samples after 105 days of curing in chemical solutions. Scanning electron microscopy (SEM) and Energy Dispersive X-Ray Analysis (EDX) were used to study the microstructural behavior and chemical element distribution of full-scale SCs. As a result, chemical attacks significantly affected upon the SC samples regarding pressure injection and jet grout's rotation parameters. In detail, the seawater solution positively impacted on the strength characteristic of SC specimens compared with the normal environment, which is the average strength has been increased 20%. While, considerable deterioration and deformation were detected in  $\text{MgSO}_4$  solution, leading to losing the mass and decreasing the strength for both parameters, ranging between -10.2% and -58.8% for mass change and 2.0 and 9.5 MPa for strength, at 105 days curing. SEM and EDX images proved the chemical attacked deteriorations and generation of hydration product with pozzolanic reactions.

**Keywords** Soilcrete column · Clayey soil · Cement · Seawater · Magnesium sulfate · Strength characteristic · SEM and EDX studies

## 1 Introduction

Numerous soil improvement methods have been used successfully in engineering practice to address a variety of geotechnical issues. Additionally, high-pressure grouting or "jet grouting" techniques were lauded for their cost-effectiveness and efficiency. The basic understanding of jet grouting is injecting controlled amounts of cement paste during small diameter nozzles on a high-pressure rotating

drill (i.e., 30–60 MPa). As well, the soilcrete (jet grout column) is cemented geometrics constructed through injecting water-cement grout and enhanced physicomaterial behaviors. The diameter of SC ranged between 40 and 140 cm depending on employed operational parameters and soil type [1]. In addition, the composition of foundation soil and the efficiency of replacing soil were indicated as considerable variables to investigate the mechanical and physical properties of high-modulus columns [2]. Besides, Water-to-cement ( $w/c$ ) ratio is represented as the main factor in controlling the mechanical behaviors of SC. Generally, the  $w/c$  ratio of 1.0 is most useful in jet grout implementations; therefore, it prefers to consider a lower  $w/c$  ratio in their substantial groundwater flow to gain on the columns with a high elasticity modulus and enhancement behavior of SC [2, 3]. Tinoco et al. [4] researched that the drilling speed & rotational velocity, pressure injection & grout volume, and time interval per step affect the geometry of the grout column. Erkan and Tan [5] evaluated the effect of rotational speed, lifting speed

✉ Hanifi Canakci  
hanifi.canakci@hku.edu.tr  
Mustafa F. Hasan  
mustafa.fahmi@epu.edu.iq

<sup>1</sup> Department of Civil Engineering, Erbil Polytechnic University, 44001 Erbil, Iraq

<sup>2</sup> Department of Civil Engineering, Hasan Kalyoncu University, 27310 Gaziantep, Turkey



**Table 1** Properties of clayey soil

Property	Values
Specific gravity (ASTM D854-10)	2.65
Water content (%)	20
Soil classification	CL
Liquid limit (%) (ASTM D4318)	28.4
Plastic limit (%)	19.9
Plastic Index (%)	8.5
Maximum dry density ( $\text{g}/\text{cm}^3$ )	1.86
Optimum moisture content (%)	13.2
Soaked CBR (%)	2.8
Standard penetration test (SPT) ( $N_{60}$ )	12
Passing sieve No. #200 (%)	62.45

of drilling rod,  $w/c$ , and injection pressure on the mechanical properties of columns in sandy soil through physical modelling. Increasing the lifting step's speed dramatically decreases the compressive strength and slightly reduces the column diameter. Furthermore, they concluded that removal of the stem at high velocity affected the uniformity of the column.

Soil development can be categorized into two major procedures. The first one, using an additive's stabilizer in the soil to increase the compacted soil's long-term strength, may take place in addition to the modification. The second one is a change in the moisture sensitivity and texture of the soil during the soil modification, which usually occurs by a change in its plasticity [6, 7]. The most common binder material used as a stabilizer to improve the performance properties of clayey soils is cement. Consequently, the stabilizing soil with cement has been detected that the unconfined compressive strength increased with the increasing percentage of cement content, reducing the plasticity index [8–11]. Sariosseiri and Muhunthan [12] indicated that the UCS of soil with low plasticity clay was enhanced five times compared with raw soil by adding 15% cement kiln dust (CKD). The soil's soaked California bearing capacity (CBR) was also enhanced by utilizing the CKD in clay soil to utilize it as a flexible pavement subgrade [13]. Another application of using soil as a construction material, Tulane et al. [14] determined that sandy clay soil is ideal for making soil–cement bricks due to its particle dispersion and sand properties. After modifying the physical properties of the soil by combining it with sand to stabilize its contents, enabling its pressing process [15].

Industrial development is the most competitive sector in the world; therefore, there were many problems involved in these activities. Thus, durability properties of cementitious material are considered as one of these problems, which OPC to chemical attacked used or released by the industrial environment. As a chemical attack, the NaCl widely

affected the geotechnical properties of kaolinite clay treated with cement kiln dust. The Atterberg limits, standard Proctor, unconfined compressive strength, and CBR tests were conducted to examine the mechanical behaviors. It was observed that using 15% CKD and 10% NaCl in clay soil reduces the  $e\text{-CO}_2$ , energy consumption, and cost of soil stabilization. In contrast, the modulus of elasticity and soil's UCS with CDK was less than cement as a stabilizer [7].

Magnesium sulfate ( $\text{MgSO}_4$ ) attack is a customary problem in the transportations, constructions, and pavements. Works of literature have notated that the durability performance of stabilized soil is significantly affected by exposing the specimens to  $\text{MgSO}_4$  solution [16–18]. After the regulated process involved in a sulfate attack, it is assumed that magnesium hydroxide and gypsum were formed as a result of the interaction between magnesium hydroxide ( $\text{MgSO}_4$ ) and calcium hydroxide ( $\text{Ca}(\text{OH})_2$ ) in the pore water. Numerous investigations have been undertaken in this field, for example, Yang et al. [19] and Little et al. [20].

Laboratory mechanical properties of SC had been observed in the works of literature according to different parameters such as the lifting speed and lifting steps. However, there is a non-similarity in geomechanical properties between the in situ and laboratory work. Therefore, this study aims to understand the durability properties of full-scale soilcrete column (SC) during injecting in the clayey soil. In addition, it has been investigated the role of pressure injection (30, 32.5, 35, 37.5, and 40 MPa) on the mass change and uniaxial strength under chemical attack's solutions (control, seawater, and  $\text{MgSO}_4$ ) of the SC that there is a lake of information in this sector. Jet grout's rotations parameter has never been considered to show the variation of geomechanics behavior; hence, this study utilized three different rotations such as 25, 35, and 45 rpm to investigate the durability and mechanical properties of full-scale samples. As emphasized earlier, the effect of pressure injection and jet grout rotations that were researched the first time for grouting in this study has been concerned with a significant gap in the previous studies. Thus, any conclusion obtained from the study results is helpful for practical application experiments.

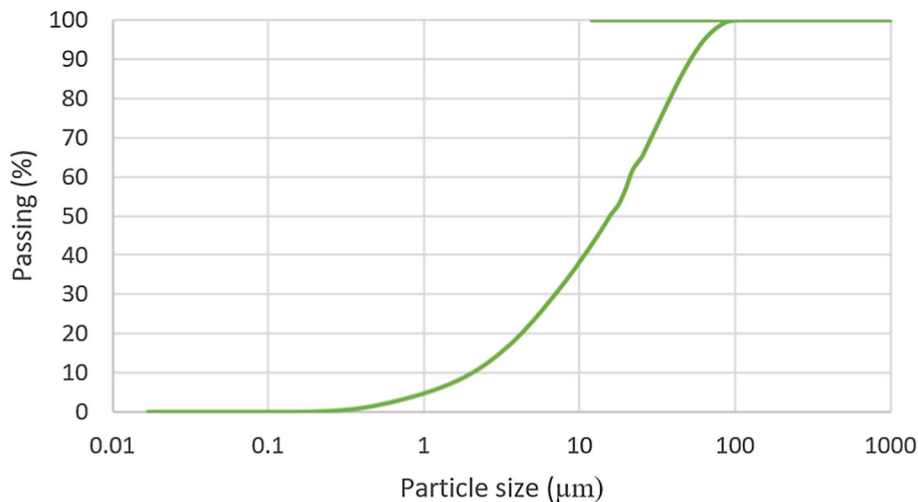
## 2 Experimental Work

### 2.1 Materials

#### 2.1.1 Soil

The soil has been utilized in this case study was clayey soil with properties that existed according to ASTM standard requirements. Soil samples taken from site work were saved in plastic bags to prevent moisture change. Based on a unified soil classification system (USCS), the soil is classified as

**Fig. 1** Particle size distribution of OPC



clayey soil (CL) with low plasticity. According to soil tests, liquid and plastic limits were 28.4% and 19.9%, respectively, and all soil properties are detailed in Table 1.

**2.1.2 Water/Cement (*w/c*)**

The full-scale SC was constructed in the site with a *w/c* ratio to analyze the durability properties in different chemical environments. Benhamou [21] reported that this range of *w/c* ratio was utilized to observe the geotechnical applications such as permeation grouting, jet-gout, and cement grout for rock or soil injection. In addition, the Portland cement used in this study is Portland cement (PC) type CEM I-42.5R according to ASTM C150 [22], which is the particle size distribution presented in Fig. 1, chemical and physical properties of PC are detailed in Table 2. Furthermore, cement paste (grout) mix has been prepared with *w/c* ratio one. In addition, the rheological properties of cement paste (grout) has been obtained by using a Coaxial rotating cylinder rheometer (ProRheo R180 Instrument, Germany), which is available in Gaziantep university – Geotechnic laboratory, as shown in Fig. 2a, b.

**Table 2** Chemical and physical properties of Portland cement (PC) of present study

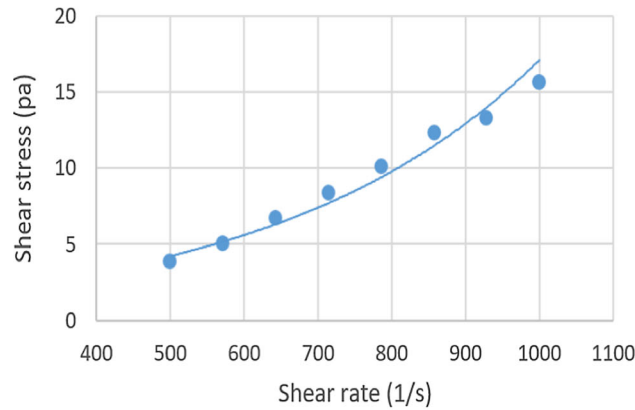
Properties	Materials	Values
Chemical (%)	CaO	61.94
	MgO	2.43
	Fe <sub>2</sub> O <sub>3</sub>	2.43
	Al <sub>2</sub> O <sub>3</sub>	5.58
	SiO <sub>2</sub>	18.08
	SO <sub>3</sub>	2.93
	Na <sub>2</sub> O	0.18
	K <sub>2</sub> O	0.99
	Loss on ignition	4.4
	Physical	Specific gravity
Fineness (Blaine)(cm <sup>2</sup> /g)		3750
d85 (85% finer size from grain size distribution curve of cement)		0.03
d95 (95% finer size from grain size distribution curve of cement)		0.07

**2.2 Jet Grout Technology In Situ Soilcrete Construction**

The technology “Jet grouting” is an injection under high pressure of various chemical reagents—binders (strengtheners) which serve to improve the properties of the soil. In this study, SC has been constructed in location Şahitkamil-Gaziantep-Turkey at 37° 08' 47.76" N and 37° 22' 24.96" E coordination as shown in Fig. 3a. In addition, after the drilling step, the injection process has been started to construct the SC by using the Comacchio MC 15 machine presented in Fig. 3b. The properties of the jet grout machine are reported in Table 3. Next, preparing cement paste in the grout mixer, which is the using Portland cement (PC) type CEM I-42.5R with

water-to-cement ratio was one. Then, grout paste has been injected with different pressure injections such as 30, 32.5, 35, 37.5, and 40 MPa in the clayey soil and different jet grout rotations, which are 25, 35, 45 rpm to construct the seven full-scale dimensions of SCs. Besides that, the case study’s jet grouting method was selected as a double fluid method. This method uses two different nozzles, which are placed opposite each other in the same rod, and from each one injected grout past and air with high pressure to erode the soil and replaced with grout past then formed the SC after hardening. Figure 4 presents the schematic diagram of SC formation procedures.

**Fig. 2** Rheological properties of jet gout column: **a** shear stress versus shear rate relationship; **b** coaxial rotating cylinder Rheometer



(a)

(b)



(a)

(b)

**Fig. 3** **a** Location of construction SC; **b** SC machine

**Table 3** Jet grouting column information

Materials	Properties
Machine name	Comacchio MC 15
Rotation (rpm)	25, 35, 45
Pullout speed (cm/min)	85 cm/min
Pressure (MPa)	30, 32.5, 35, 37.5, 40
Cement type	Cem I, 42.5 R
W/C	1:1
Viscosity (s/l)	33 s/1000 ml
Fluidity of concrete	70%

### 2.3 Sample Preparation

This section covers the preparation of the test specimen after casting a full-scale SC (Grouting column) in the clayey soil.

Next, the grouting column has been cured in the clayey soil for 28 days. After that, the area around the column was excavated to extract full-scale dimensions and transported to the geotechnical laboratory belonging to Gaziantep University – Turkey, and taking a core sample was then covered with plastic sheets to protect the moisture of the sample, as shown in Fig. 5a–c. After preparing the test specimens, the size of specimens was prepared with 50\*100 mm according to ASTM D698. For each condition (control, seawater, MgSO<sub>4</sub>), a total of eight samples were designed regarding pressure injection and rotation’s parameters, and three samples at each parameter were used for work accuracy; therefore, a total of 72 samples were prepared to cover this study. All samples were exposed to different chemical environments, such as seawater (NaCl) and magnesium sulfate (MgSO<sub>4</sub>) solutions, to study the durability properties of full-scale SC. The test samples are labelled according to different pressure injections such as 30, 32.5, 35, 37.5, and 40 MPa with three different jet

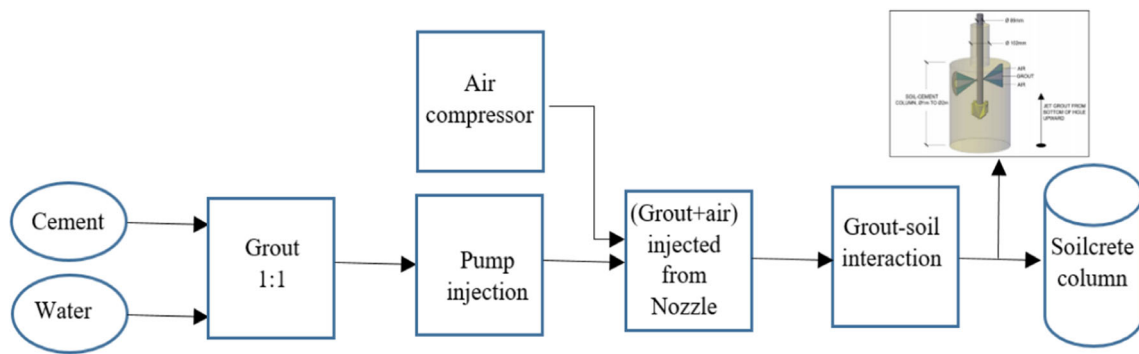


Fig. 4 Schematic diagram of SC procedure formation



(a)

(b)



(c)

Fig. 5 SC samples, a coring samples, b covering with a plastic sheet, c labeling the samples

**Table 4** Experimental program of the study

Sample code	w/c	Pressure injection (MPa)	Jet grout's rotation (rpm)	Water content (%)
SC30-35	1:1	30	35	28
SC32.5-35	1:1	32.5	35	29
SC35-35	1:1	35	35	28
SC37.5-35	1:1	37.5	35	28
SC40-35	1:1	40	35	29
SC40-25	1:1	40	25	32
SC40-35	1:1	40	35	29
SC40-45	1:1	40	45	22

grout's rotations (25, 35, 45) rpm. Therefore, the test sample has been labelled as SC30-35, which means that the (SC) is a soilcrete specimen, the pressure injection is 30 MPa, and the jet grout's rotation is 35 rpm, as detailed in Table 4.

## 2.4 Test Methods

### 2.4.1 Chemical Attacks Test

Durability properties exposed to chemical attacks of SC according to ASTM C267 – 01 requirements [23]. However, there is no specific test method to evaluate the durability of concrete exposed to chemical attacks. In this study, magnesium sulfate ( $MgSO_4$ ) with a concentration of 1% by weight and sodium chloride (seawater) (NaCl) with a concentration of 3.5% by weight was prepared, and the specimens were fully soaked in the chemical solution for 105 days. Before the chemical exposure, the specimens were immersed in water for 24 h and then left to dry for 2 h at  $23 \pm 2$  °C to determine the initial weight of the specimens. At the end of each week of exposure time, the specimens were removed from the chemical solution tank and washed with water to eliminate chemical reaction products remaining on the surface of the specimens. The specimens were then left to dry at  $23 \pm 2$  °C for 2 h before measuring their weights. Deterioration level and change in the surface of specimens were also evaluated by visual observation after each week of exposure. After each week, the cumulative change in weight for each test specimen was determined using the following formula:

$$M_c = \frac{W_t - W_i}{W_i} * 100$$

where  $M_c$  is the cumulative change in weight from initial to weight at time  $t$ ,  $W_i$  is the initial weight of the specimen before immersing in the chemical solution (in grams),  $W_t$  is the weight of the specimen at time  $t$  (in grams).



**Fig. 6** Unconfined compression test machine

### 2.4.2 Unconfined Compressive Strength (UCS)

The UCS test was examined on the soilcrete samples to measure the strength value of specimens before and after chemical attack for comparison and evaluate the degree of chemically attacked affection after 105 days curing according to different pressure injection and jet grout's rotations parameters. The procedure test followed the ASTM D2166 [24] requirements. Therefore, it placed the samples in the center of the device and adjusted the loading machine carefully till touch the sample's surface, then recorded zero as shown in Fig. 6. Afterward, apply the load with axial strain at a 0.5–2.0% /min rate. Note the strain rate should be chosen so that the time to failure does not exceed about 15 min.

### 2.4.3 SEM and EDX Test

Figure 7 presents the Gemini300 (ZEISS) machine scanning electron microscopy (SEM) machine used to analyze the changes in the interfacial transition zone between cement and clayey soil regarding pressure injection and jet grout rotations before and after exposure to chemical attack. Energy

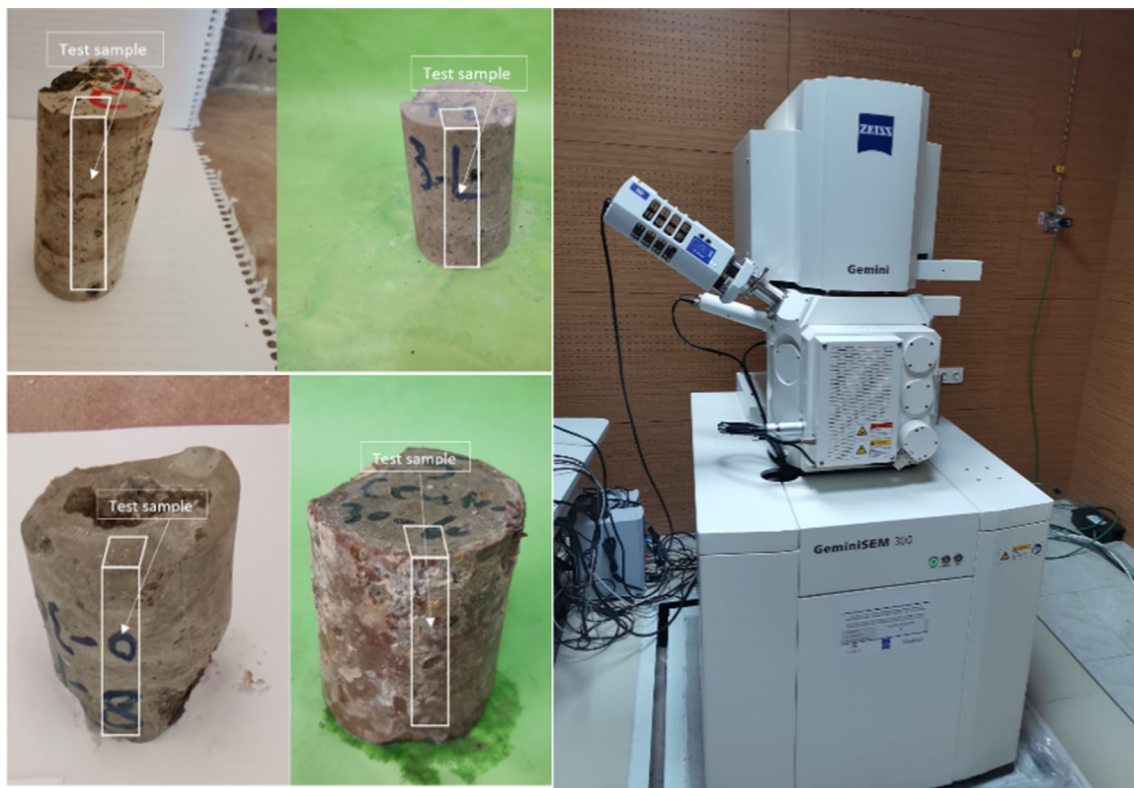


Fig. 7 SEM and EDX image machine

Dispersive X-Ray Spectrometer (EDX) image was also examined to the specimens by Oxford Instruments, supported by Aztec software, which is present in the central laboratory of Gaziantep University to show any change in chemical elements composition of SC. The sample section is located from the samples' outermost layer (maximum 1 cm from the outer layer). One inch (2.54 cm) slice of the specimens was cut and discarded from both bottom and top regions and a 1-cm-thick rectangular slice from the middle sections of the samples.

### 3 Result and Discussion

#### 3.1 Chemical Attacks

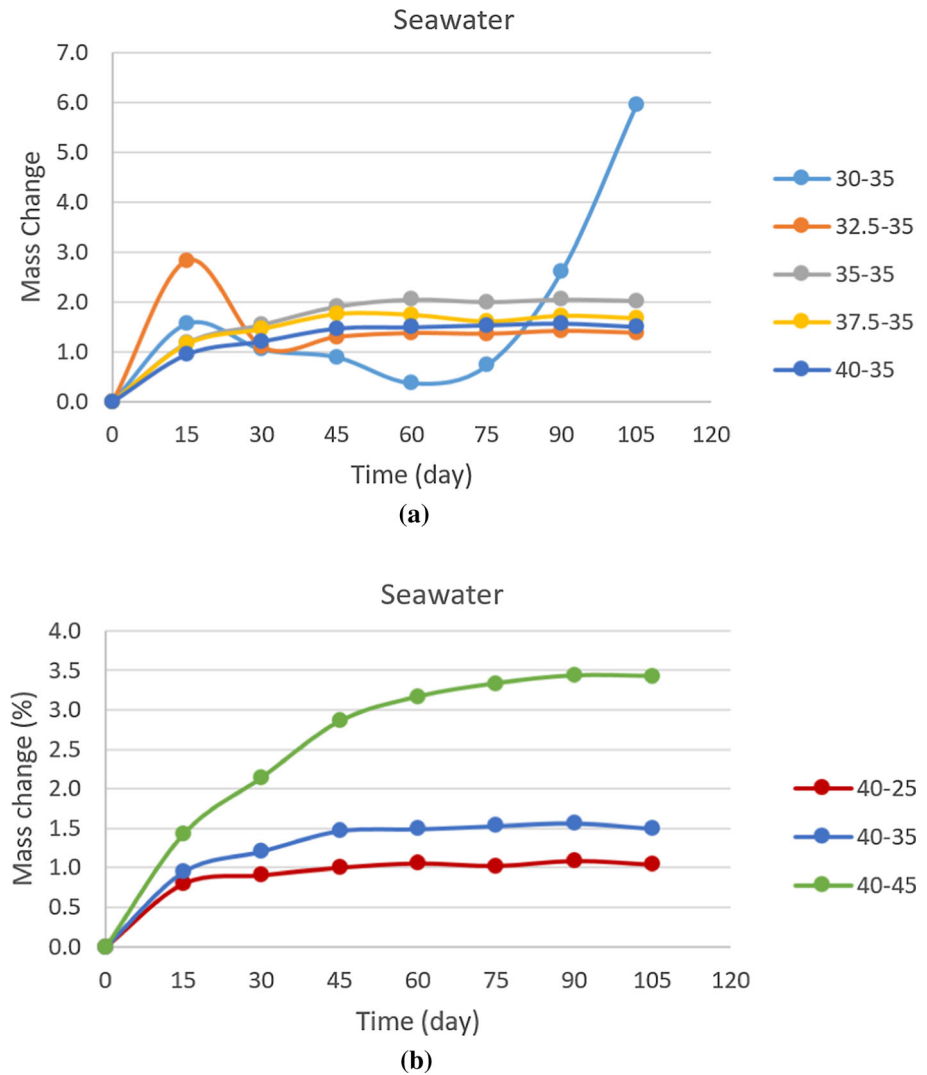
##### 3.1.1 Mass Change of SC

According to pressure injection and jet grout rotations, mass change of SC has been observed after 105 days from different environments, such as seawater (3.5%) and magnesium sulfate ( $\text{MgSO}_4$ ) with a constant solution concentration of 1%.

**Seawater (NaCl)** Figure 8a, b illustrates the mass change of soilcrete sample exposed to 3.5% seawater solution regarding pressure injection and jet grout's rotations, respectively. The

change in mass was calculated for all samples in the control environment through constant hydration [25, 26]. Generally, the mass change investigated variation due to exposure in seawater solutions, while the sample's surface has not been deformed compared with normal conditions. In addition, variation of mass changes has been fixed after 45 days of immersing in solution for most parameters of pressure injection, as shown in Fig. 8a. The optimum mass change has been achieved at sample SC30-35, which is 6% for 105 days and 0.9% for 45 days; therefore, it can be concluded that there is a significant change with the 30 MPa pressure injection and 35 rpm rotations. Additionally, it indicates that the porosity is large in comparison with other metrics, meaning that the permeability and chemical absorption are increased [27]. 1.3%, 1.9%, 1.8%, and 1.5% were considered as percentage of mass change of samples SC32.5-35, SC35-35, SC37.5-35, and SC40-35, respectively. The weight gain due to absorption of the chemical solution was also reported by several works of literature [28, 29]. Sanni and Khadiranaikar [30] concluded weight loss of normal concrete specimens under 5% magnesium sulfate and 3.5% seawater environment were 0.43% and 0.35%, respectively, as well, the present study was observed that the seawater had less effect on the soilcrete sample compared with other chemical attacked. The results of jet grout rotations detected a significant variation in jet grout columns. The mass change was stable after 45 days for

**Fig. 8** Mass change of SC exposed in seawater, **a** pressure injections, **b** jet gout rotations

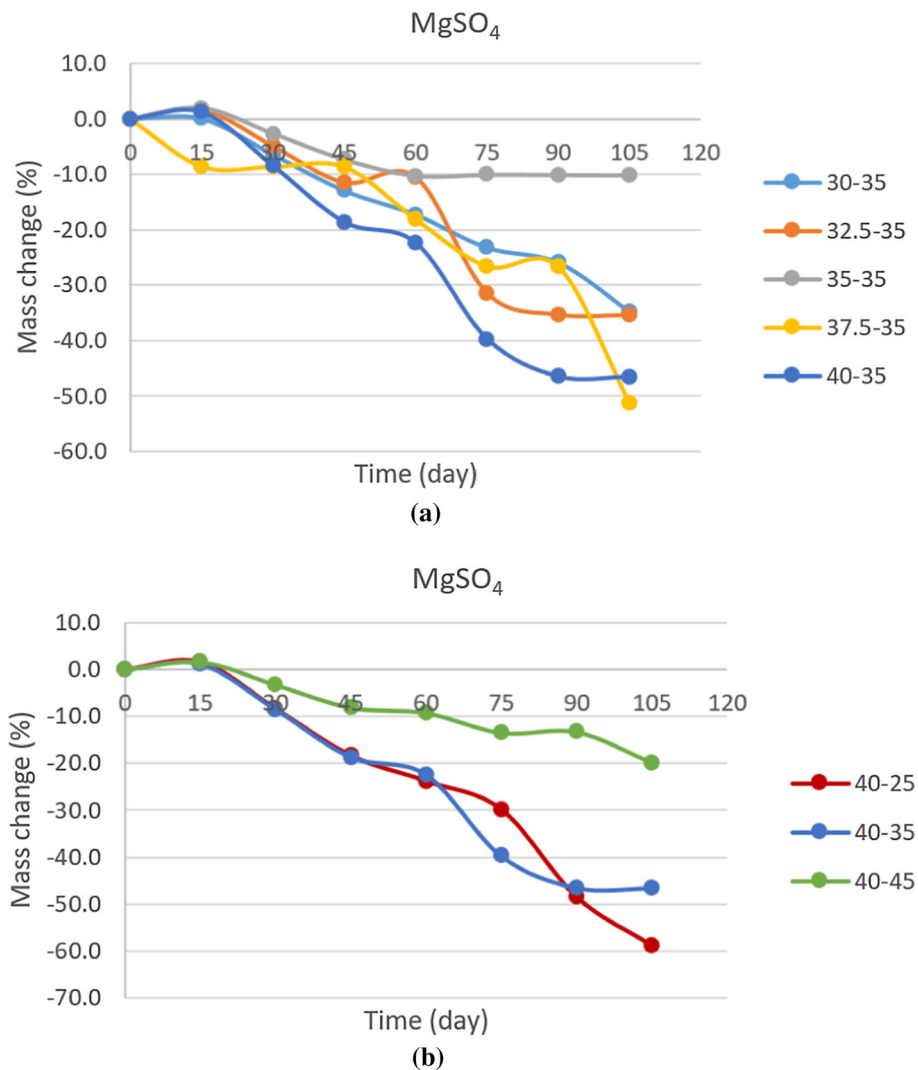


samples SC40-35 and SC40-25, while the mass change of SC40-45 continuously increased with increasing the curing time to 105 days; it can be attributed that the clay content covers the large space of sample that caused to high permeability and chemical absorption. Furthermore, specimen SC40-45 was recorded optimum value of mass change which is exceeded 2.9% for 45 days and 3.4% for 105 days, which indicates that the sample contained higher porosity and less density compared with SC40-25 and SC40-35, that leads to increasing the chemical absorption and high permeability. While, the minimum result has been achieved at soilcrete sample 40-25 which is 0.8% and 1% for 15 and 105 days, respectively, it means with the less rotation leads to exist the pure soilcrete with less porosity, less chemical absorption, and high density. Besides that, the variation of mass change has been fixed for sample 40-35 and 40-25 after 45 days exposing as shown in Fig. 8b.

**Magnesium Sulfate ( $MgSO_4$ )** This study also presented the affection of magnesium of sulfate ( $MgSO_4$ ) on soilcrete samples. Figure 9a, b reports that the pressure injections and jet grot rotations significantly affect the mass change of soilcrete samples. Generally, Mass change detected a significant variation due to exposure of the SC samples to 1% sulfate solutions. The rate of decrease was not uniform and ranged between 10 and 47% for pressure injections and 20–47% for rotations. It can be understood that cement grot of sample heterogeneously distributed in clayey soil. The decrease in weight was observed for all specimens at all pressure injections, which is detailed in Fig. 9a. However, the reduction rate was more remarkable than seawater because the C–S–H rapidly loses calcium (Ca) ions and transforms them into magnesium silicate hydrates ( $Mg-S-H$ ). Therefore, its non-binding compounds are generated when magnesium hydroxide reacts with silica gel [31–33]. In this case, specimen SC35-35 was notated as a minimum value of mass change for 45 and 105 days, which are – 7.4% and –



**Fig. 9** Mass change of SC exposure to  $MgSO_4$ , **a** pressure injections, **b** jet grout rotations



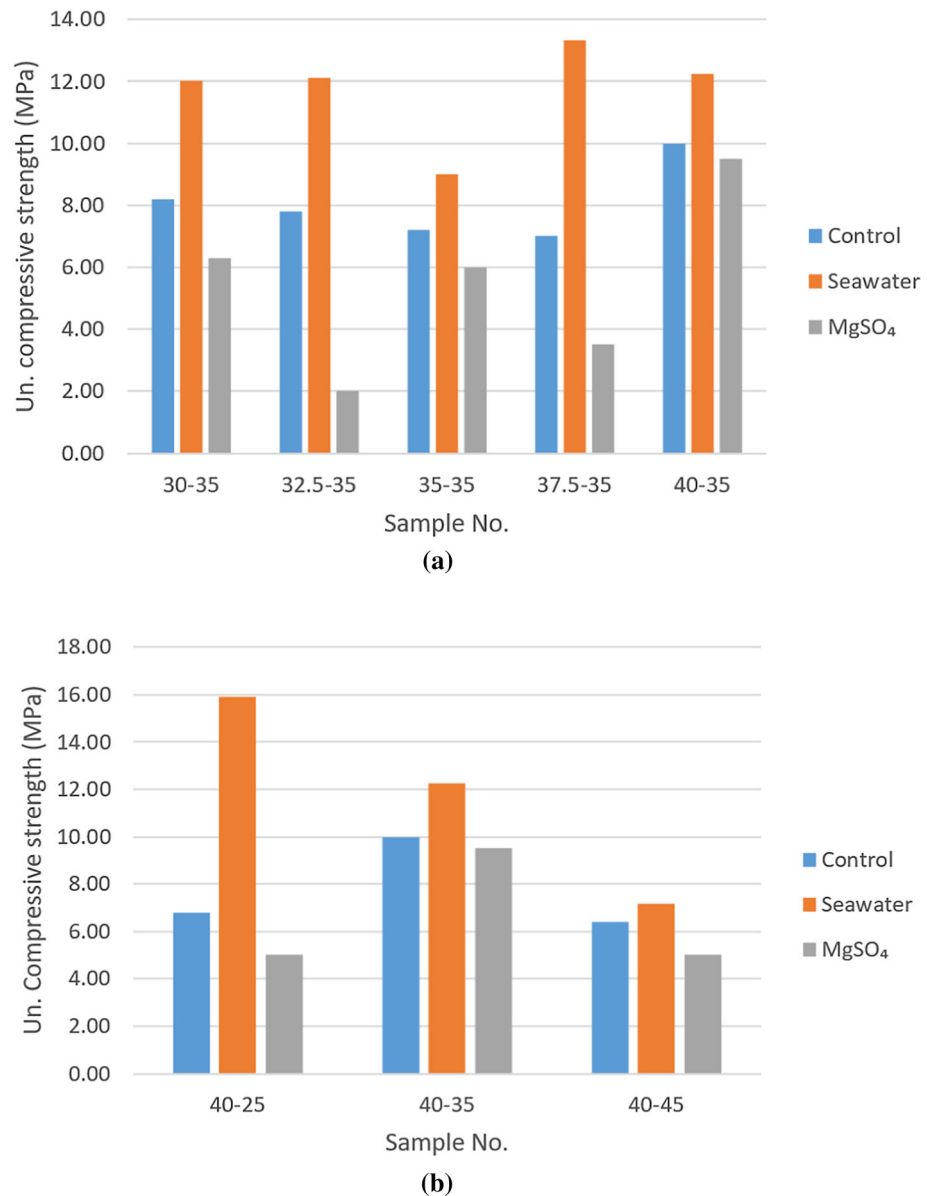
10.2%, respectively, and the results are very high compared with the seawater. While the highest mass change has been reached at samples SC37.5-35 and SC40-35 for all ages, it can be attributed that the samples consist of a large amount of cement content that leads to increasing the pozzolanic reaction and generation hydration products [34].

The jet grout’s rotations observed a significant effect on the SC during exposure to  $MgSO_4$  solution with a concentration of 1%. As a result, sample SC40-45 is considered a minimum result compared with 40-25 and 40-35, which are – 19.8%, – 58.8%, and 46.5%, respectively, for 105 days curing, as shown in Fig. 9b. It is considered that the results are acceptable compared with previous studies, and the weight gain at the first 30 days due to absorption of magnesium sulfate solution was also reported in this case study which has the same manner as the previous studies [28, 29]. Cordon [35] concluded that the soilcrete is subject to the attack of sulfate much in the same manner as concrete, but deterioration in soilcrete is more rapid than cement concrete.

Reactions between the cement and chemical solution lead to reducing the density of concrete due to the formation of ettringite ( $C_4A_3S$ ) and gypsum ( $CaSO_4$ ) [36, 37]. However, the initial weight gains of the specimens may result from the lower reduction amount in relative density than the increase in relative volume [36].

**Compressive Strength Approach** This study presented the uniaxial strength of SC in different environments such as control (No attacked), seawater (NaCl), and magnesium sulfate ( $MgSO_4$ ) regards with different pressure injection and jet grout’s rotations, as shown in Fig. 10a, b. According to the results, the chemical attack wildly affected the soilcrete samples. However, the strength of specimens after being immersed in  $MgSO_4$  solution recorded the maximum results compared to control, seawater for all pressure injections and jet grout’s rotations. In detail,  $MgSO_4$  solution has a considerable influence and high deformation on the SC in pressure injection. after being exposed to seawater solution,

**Fig. 10** Compressive strength of SC at different environments, **a** pressure injections, **b** jet grout's rotations



the optimum result has been recorded at soilcrete samples SC37.5-35, which is 13.31 MPa, compared with specimens SC30-35, SC32.5-35, SC35-35, and SC40-35 were 12.0, 12.1, 9.0, and 12.24 MPa, respectively, as shown in Fig. 10a. It can be understood that the percentage of cement generally increased with increasing the pressure and caused to rising the strength. Besides that, the SC exposure to seawater improves the strength performance of cement paste binder by producing calcium-sodium silicate gel through the combination of cement calcium and dissolved silicate of the clay structure [38]. According to jet grout rotations, the results concluded that the minimum and maximum strength had been measured at specimens SC40-35 and SC40-25, 7.17 and 15.89 MPa, respectively, as presented in Fig. 10b. This

variation in strength means that the rotations have a significant effect on the uniaxial strength. The percentage of cement increased with decreasing the rotation, which increased the strength. Ghavami et al. [7] also concluded that the maximum stress of cement-soil specimen was obtained by increasing the percentage of NaCl. It can be understood this increasing related to producing of continuous pozzolanic reactions throughout curing time. As seen, the maximum compressive strength increased by 18% with adding 10% NaCl to cement-kaolinite clay soil compared with NaCl-free sample throughout 7 days of curing time. In addition, the calcium-sodium silicate gel was produced because of the combination of dissolved silicate of the clay structure and cement calcium that improves the strength properties of specimens. Afterwards, soilcrete specimens behave more brittle compared

with non-salt soil. In conclusion of the present study, the strength of the soilcrete sample enhanced after exposure to seawater solutions.

The SC significantly deformed due to exposure to  $MgSO_4$  solution because of reaction has been occurred with cement. As seen, the maximum strength obtained as specimen SC40-35 for both pressure injection and rotation's parameter compared with SC30-35, SC32.5-35, SC35-35, SC37.5-35, SC40-25, and SC40-45 were 6.3, 2.0, 6.0, 3, 5.0, and 5.0 MPa, respectively. Based on the literature's results, the minimum compressive strength value of the specimen was observed after exposure to 1% concentration of magnesium sulfate ( $MgSO_4$ ) solutions compared with the strength of the specimen immersed in water for one day. In addition, the  $MgSO_4$  solution was more effective (loss strength, deformation, visual appearance degradation) on the SC specimens than sodium sulfate solution at the same concentration of solutions and regardless of the type of cement. In detail,  $MgSO_4$  salt is more aggressive than sodium sulfate, which leads to more harm and deterioration on specimens. It can be understood that this influence was causing the crack formation and expansion during the sulfate attack and evanishing the calcium silicate hydrate's binding property and the cement [39]. Additionally, the decrease in strength of specimens after exposure to  $MgSO_4$  solution indicates that the calcium ion in calcium silicate hydrate (C-S-H) has been replaced by magnesium, then resulting in magnesium silicate hydrate (Mg-S-H), which is detrimental to the bonding forces within the composite or non-binding materials [33, 34, 40].

### 3.2 Visual Appearance

#### 3.2.1 Specimens Exposed to the 1% Seawater (NaCl) Solution

Throughout this study, it was observed that the sodium chloride (seawater) significantly affected SC by testing the change in mass and compressive strength and evaluating the change in visual appearance of the sample. Figure 11 shows the change of visual appearance of soilcrete samples before and after curing 105 days in 1% seawater's solution, which concluded that the best technique to assess the SC's degradation is to monitor the visual appearance and measure the mass change of the test specimens. As seen, the color change has been observed for all specimens compared with the control sample. According to the structure of a sample, all specimens were not deformed after immersing samples for 105 days in sodium chloride solution. The same findings were observed from previous research [27].

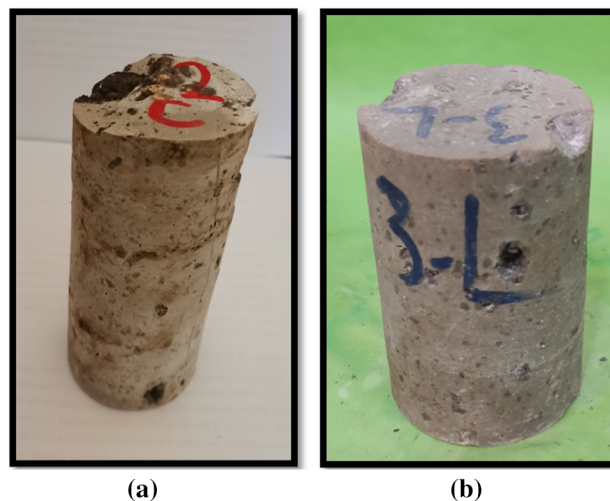


Fig. 11 Visual appearance of SC exposed to seawater for 105 days, a before curing, b after curing

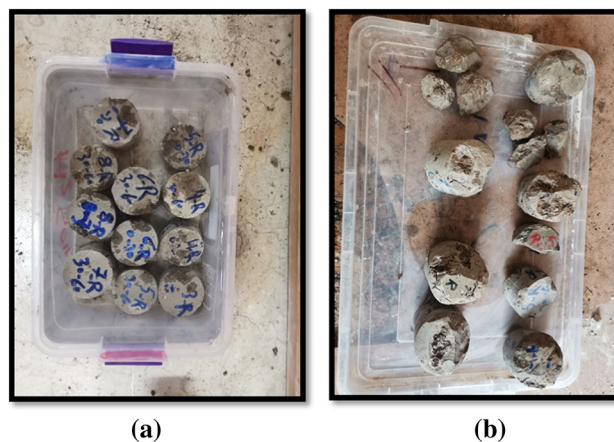


Fig. 12 Visual appearance of SC exposed to  $MgSO_4$  solution for 105 days, a before curing, b after curing

#### 3.2.2 Specimens Exposed to the 1% Magnesium Sulfate ( $MgSO_4$ ) Solution

Figure 12 shows the visual appearance of SC that was exposed to a 1% concentration of  $MgSO_4$  solution for 105 days. Besides that, samples' mechanical and physical properties have also been significantly changed after being exposed to the chemical solution. According to the results, most cracks and deterioration in the shape of soilcrete specimens occurred when exposed to magnesium sulfate solution, which depends on the presence of cement content that leads to break up to small parts of SC and do not revert to original features of soil [35]. This study concluded that the maximum deterioration and deformation have occurred in soilcrete samples exposed to  $MgSO_4$  solution compared with seawater.

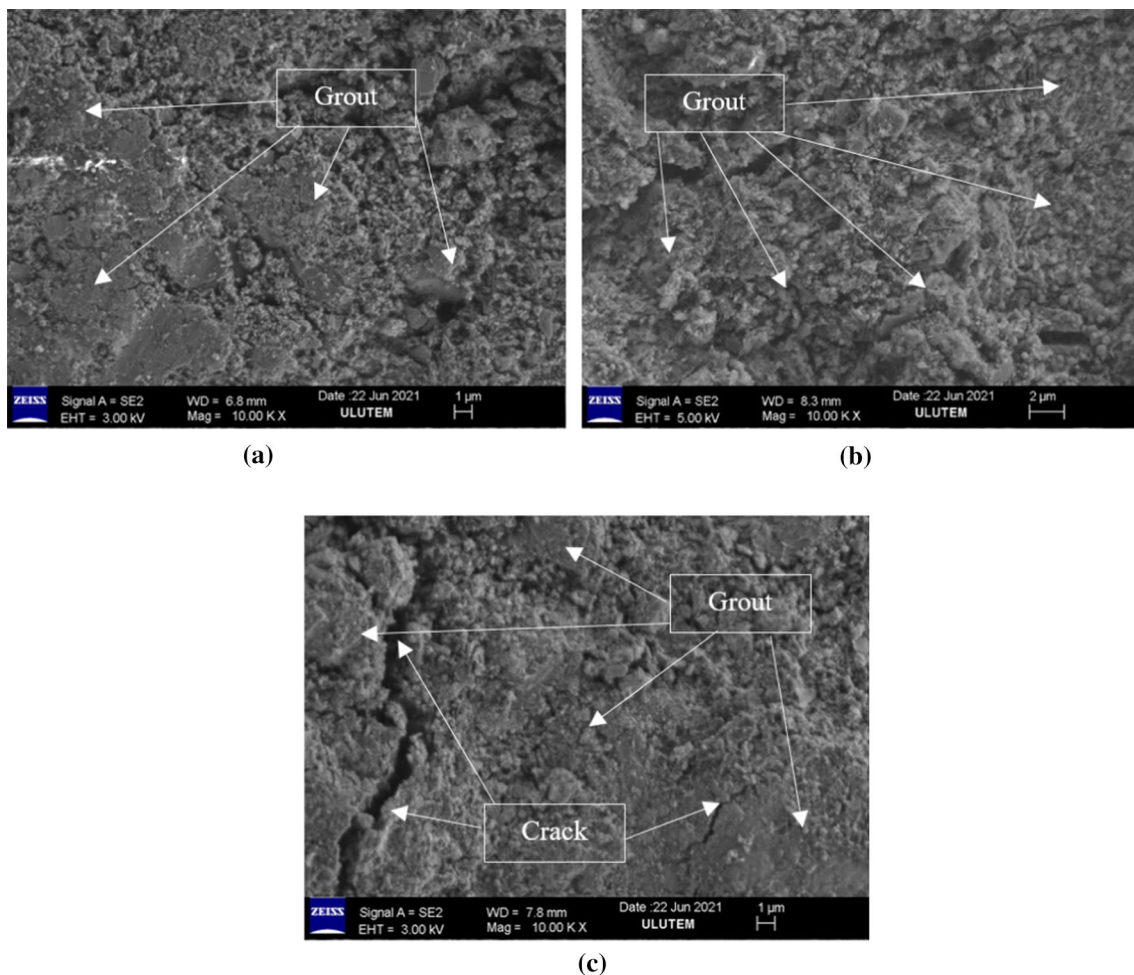


Fig. 13 SEM analysis of SC in different environments, **a** control, **b** seawater, **c**  $\text{MgSO}_4$

### 3.3 Microstructural Studying of SC

#### 3.3.1 SEM Analysis

SC was analyzed in detail by scanning electron microscopy (SEM) to observe the variation in the interfacial transition zone (ITZ) between the grout materials and clay soil after the chemical attack (control, seawater, and  $\text{MgSO}_4$ ) for 105 days curing as detailed in Fig. 13a–c. Due to the fact that all chemical attacks occur at the surface of the samples, deformation begins at the surface and progresses to the interior [36]. SEM photos have been possessed for all specimens after exposure to chemicals attacked from the samples' outermost layer (maximum 1 cm from the outermost layer). One inch (2.54 cm) slices of the specimens were slit and discarded from both bottom and top regions and 1 cm thick circular slice from the middle sections of the samples then scanned by SEM test at magnification 10,000 times. Figure 13a, b shows the SEM analysis of soilcrete samples at normal and seawater conditions, as well, the samples had not been deformed according

to the structure after 105 days curing. While the seawater solution has been wildly affected the specimen's surface according to the color as presented in Fig. 11. Figure 13c illustrates the SEM analysis of soilcrete specimen after exposure to  $\text{MgSO}_4$  solution, and it was detected that the  $\text{MgSO}_4$  more aggrieve the normal and seawater conditions. Therefore, the surface's deterioration appears on the specimen due to the structure and colors, then caused to expansion and cracked formation during the sulfate attack and demising of binding property of cement and calcium silicate hydrate as well [39].

#### 3.3.2 EDX Analysis

The EDX was used to classify the chemical compositions of soilcrete specimens subjected to various chemical conditions, including normal, saltwater (NaCl), and magnesium sulfate ( $\text{MgSO}_4$ ) solution (Fig. 14a–c). Additionally, this approach blasted electrons in the desired region of elemental composition. The chemical elements will then release

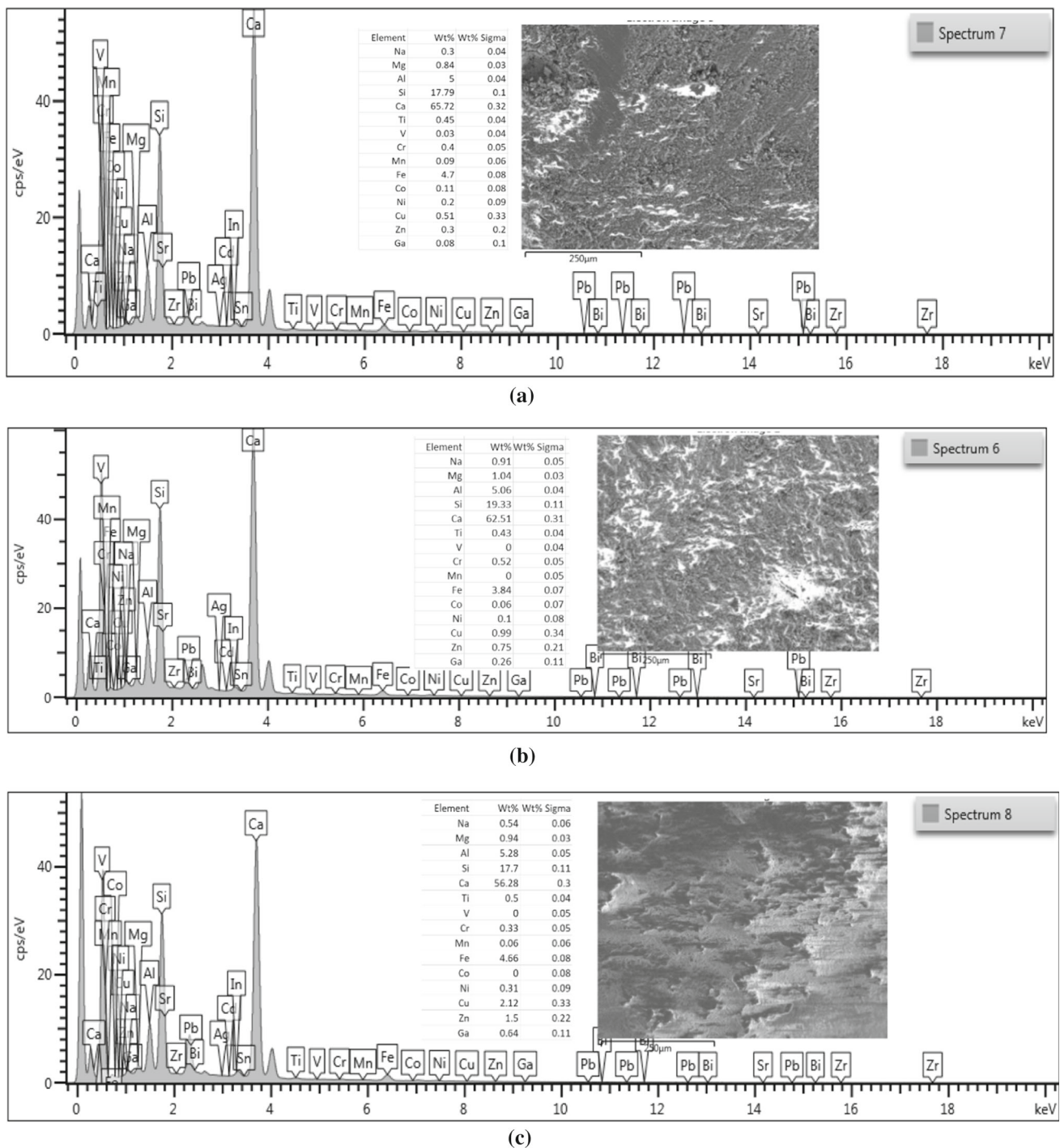


Fig. 14 EDX analysis of SC after exposure to different chemical environments, a normal, b seawater, c MgSO<sub>4</sub>

distinctive X-rays, which may be detected on the detector [41]. To illustrate any differences in chemical elements, content, and structure of SC, an EDX image was taken using the Gemini300 machine. Additionally, Fig. 14a depicts the EDX picture of the soilcrete sample in its natural state. The cement grout injected into the clayey soil has a high concentration of

cement, which results in the highest concentrations of chemical components such as calcium (Ca) and iron (Fe) compared to a chemically attacked specimen, which is 62.75% and 4.7%, respectively. However, Si (17.79%) and Al (5%) were considered due to the presence of soil in the samples. In Fig. 14b, the micrograph of the soilcrete sample after exposure to NaCl solution is finished. As can be observed, the

(Ca) chemical element peak remains visible compared to a normal situation due to a considerable quantity of Ca at this location. Therefore, it is indicated that C–S–H may occur in the same area; hence, this pozzolanic reaction fills the pore space of clay, increasing its strength and geotechnical qualities [42]. Figure 14c illustrates the EDX examination of a soilcrete sample after being soaked in a 1% MgSO<sub>4</sub> solution. As shown by the result, the specimen lacked cementitious components, and ettringite formation occurred, although the clay's shape remained consistent. Thus, Ca was reduced by 14% compared to a normal situation. Simultaneously, the Si and Al contents were still rising at 17.7% and 5.28%, respectively. Additionally, this reaction forms silicium, aluminum, and ferric oxide hydrogels [43]. Thus, the identical results reported in this investigation indicated that the Ca element was reduced by more than 43% compared to the natural environment.

## 4 Conclusion

This paper observed the influence of pressure injection and jet grout's rotation on SC's strength and durability properties in clayey soil. The durability properties of SC were analyzed, and the following conclusion was drawn:

- This study detected that the mass change investigated variation due to exposure in seawater solutions, while the sample's surface has not been deformed compared with normal conditions. The maximum mass change has been obtained at a sample SC30-35, which is 6% for 105 days and 0.9% for 45 days. The results of jet grout rotations detected a significant variation in jet grout columns. The mass change was stable after 45 days for samples SC40-35 and SC40-25 (1% and 1.5%), while the mass change of SC40-45 continuously increased with increasing the curing time, which is 3.4% after 105 days of curing.
- Magnesium sulfate attack is considered an effective parameter on the SC regarding pressure injection and rotations. Therefore, the variation of mass change ranged between 10 and 47% for pressure injection and 20–47% for rotations, which is very high compared with the seawater attacked. The maximum mass reduction has been exceeded – 51.2% and – 46.5% at samples SC37.5-35 and SC40-35 for all ages. The same approach of mass change was observed according to jet grout rotations after 105 days of curing.
- Strength properties of full-scale SC after chemical attached also investigated a wild variation regarding pressure injection and jet grout column. Therefore, the strength of specimens after being immersed in MgSO<sub>4</sub> solution recorded the minimum results compared to control and seawater environments, which ranged between 0.0 and 9.5 MPa.

According to the control environment, the strength value was varied from 6.2-to-10.0 MPa for both pressure injection and rotation and ranged between 7.17 and 15.89 MPa for seawater conditions.

- SEM and EDX results of full-scale SC observed the reaction of chemical solution with the samples, and generation of hydration products increased with increasing chemical curing time. It is also proved the variation of durability and mechanical properties. Generally, MgSO<sub>4</sub> solution observed the highly surface deteriorations and structural deformation of soilcrete samples after curing for 105 days curing compared with normal and seawater environments.
- Future investigation on the presenting more durability properties of SC through subjecting to the sulfuric acid (H<sub>2</sub>SO<sub>4</sub>) solution, considered a chemical attack and wetting and drying test. Besides that, it is recommended to improve the geomechanical properties of Full-scale SC column using different methods and different binder materials to replace cement such as silica fume, slag, and fly ash. More investigation about laboratory working compared with site working because of the heterogeneous distribution of soil.

**Acknowledgements** The experimental study of the present paper was conducted at the Civil Engineering Laboratory of the University of Gaziantep through the PhD thesis of the First author. The authors would like to present their gratitude to the anonymous reviewers for carefully reviewing the manuscript and providing valuable comments.

## References

1. Lunardi, P.: Ground improvement by means of jet-grouting. *Proc. Inst. Civ. Eng. Improv.* **1**, 65–85 (1997)
2. Croce, P.; Flora, A.; Modoni, G.: *Jet Grouting: Technology, Design and Control*. CRC Press (2014)
3. Akan, R.; Keskin, S.N.; Uzundurukan, S.: Multiple regression model for the prediction of unconfined compressive strength of jet grout columns. *Procedia Earth Planet. Sci.* **15**, 299–303 (2015)
4. Tinoco, J.; Correia, A.G.; Cortez, P.: Jet grouting mechanicals properties prediction using data mining techniques. In: *Grouting and Deep Mixing 2012*, pp. 2082–2091 (2012)
5. Erkan, İ.H.; Tan, Ö.: The effect of pulling and rotation speed on the jet grout columns. *Int. J. Civ. Environ. Eng.* **10**, 1690–1694 (2017)
6. Parsons, R.L.; Johnson, C.P.; Cross, S.A.: *Evaluation of soil modification mixing procedures*. Department of Transportation, Kansas (2001). <https://rosap.nrl.bts.gov/view/dot/14515>
7. Ghavami, S.; Jahanbakhsh, H.; Azizkandi, A.S.; Nejad, F.M.: Influence of sodium chloride on cement kiln dust-treated clayey soil: strength properties, cost analysis, and environmental impact. *Environ. Dev. Sustain.* **23**, 683–702 (2020)
8. Basha, E.A.; Hashim, R.; Mahmud, H.B.; Muntohar, A.S.: Stabilization of residual soil with rice husk ash and cement. *Constr. Build. Mater.* **19**, 448–453 (2005)
9. Al-Rawas, A.A.; Hago, A.W.; Al-Sarmi, H.: Effect of lime, cement and Sarooj (artificial pozzolan) on the swelling potential of an expansive soil from Oman. *Build. Environ.* **40**, 681–687 (2005)

10. Sariosseiri, F.; Muhunthan, B.: Effect of cement treatment on geotechnical properties of some Washington State soils. *Eng. Geol.* **104**, 119–125 (2009)
11. Asgari, M.R.; Dezfouli, A.B.; Bayat, M.: Experimental study on stabilization of a low plasticity clayey soil with cement/lime. *Arab. J. Geosci.* **8**, 1439–1452 (2015)
12. Sariosseiri, F.; Muhunthan, B.: Geotechnical properties of Palouse loess modified with cement kiln dust and Portland cement. In: *GeoCongress 2008: Characterization, Monitoring, and Modeling of GeoSystems*, pp. 92–99 (2008)
13. Sharma, R.K.: Laboratory study on stabilization of clayey soil with cement kiln dust and fiber. *Geotech. Geol. Eng.* **35**, 2291–2302 (2017)
14. da Silva, T.R.; Cecchin, D.; de Azevedo, A.R.G.; Valadão, I.; Alexandre, J.; da Silva, F.C.; Marvila, M.T.; Gunasekaran, M.; Garcia-Filho, F.; Monteiro, S.N.: Technological characterization of PET—polyethylene terephthalate—added soil-cement bricks. *Materials (Basel)* **14**, 5035 (2021)
15. Azevedo, A.R.G.; Marvila, T.M.; Fernandes, W.J.; Alexandre, J.; Xavier, G.C.; Zanelato, E.B.; Cerqueira, N.A.; Pedroti, L.G.; Mendes, B.C.: Assessing the potential of sludge generated by the pulp and paper industry in assembling locking blocks. *J. Build. Eng.* **23**, 334–340 (2019)
16. Obika, B.; Freer-Hewish, R.J.: Soluble salt damage to thin bituminous surfacings of roads and runways. *Aust. Road Res.* **20**(4), 3–12 (1990)
17. Rajasekaran, G.; Murali, K.; Srinivasaraghavan, R.: Effect of chlorides and sulphates on lime treated marine clays. *Soils Found.* **37**, 105–115 (1997)
18. Yi, Y.; Li, C.; Liu, S.; Jin, F.: Magnesium sulfate attack on clays stabilised by carbide slag-and magnesia-ground granulated blast furnace slag. *Geotech. Lett.* **5**, 306–312 (2015)
19. Yang, Y.; Wang, G.; Xie, S.: Effect of magnesium sulfate on the unconfined compressive strength of cement-treated soils. *J. Test. Eval.* **40**, 1244–1251 (2012)
20. Little, D.N.; Nair, S.; Herbert, B.: Addressing sulfate-induced heave in lime treated soils. *J. Geotech. Geoenviron. Eng.* **136**, 110–118 (2010)
21. Benhamou, J.-P.: Indications for liver transplantation in primary biliary cirrhosis. *Hepatology* **20**, S11–S13 (1994)
22. ASTM, A: C150/C150M-17, Standard Specification for Portland Cement. Am. Soc. Test. Mater., West Conshohocken (2017)
23. Concretes, P.: Standard test methods for chemical resistance of mortars, grouts, and monolithic. *Current* **04**, 1–6 (1998)
24. ASTM: Standard Test Method for Unconfined Compressive Strength of Cohesive Soil, Vol. 4, p. 1–7. ASTM Int. (2013)
25. Li, Z.; Ding, Z.: Property improvement of Portland cement by incorporating with metakaolin and slag. *Cem. Concr. Res.* **33**, 579–584 (2003)
26. Li, S.; Roy, D.M.: Preparation and characterization of high and low CaO/SiO<sub>2</sub> ratio “pure” C-S-H for chemically bonded ceramics. *J. Mater. Res.* **3**, 380–386 (1988)
27. Alzebaree, R.; Çevik, A.; Mohammedameen, A.; Niçş, A.; Gülşan, M.E.: Mechanical performance of FRP-confined geopolymer concrete under seawater attack. *Adv. Struct. Eng.* **23**, 1055–1073 (2020)
28. Thokchom, S.: Fly ash geopolymer pastes in sulphuric acid. *Int. J. Eng. Innov. Res.* **3**, 943–947 (2014)
29. Wallah, S.; Rangan, B.V.: Low-calcium fly ash-based geopolymer concrete: long-term properties. Curtin University of Technology, Perth, Australia (2006). <http://hdl.handle.net/20.500.11937/34322>
30. Sanni, S.H.; Khadiranaikar, R.B.: Performance of geopolymer concrete under severe environmental conditions. *Int. J. Civ. Struct. Eng.* **3**, 396–407 (2012)
31. Santhanam, M.; Cohen, M.D.; Olek, J.: Mechanism of sulfate attack: a fresh look: part 1: summary of experimental results. *Cem. Concr. Res.* **32**, 915–921 (2002)
32. Santhanam, M.; Cohen, M.D.; Olek, J.: Mechanism of sulfate attack: a fresh look: part 2. Proposed mechanisms. *Cem. Concr. Res.* **33**, 341–346 (2003)
33. Lee, K.-M.; Bae, S.-H.; Park, J.-I.; Kwon, S.-O.: Mass change prediction model of concrete subjected to sulfate attack. *Math. Probl. Eng.* (2015). <https://doi.org/10.1155/2015/298918>
34. Chegenizadeh, A.; Keramatikerman, M.; Panizza, S.; Nikraz, H.: Effect of powdered recycled tire on sulfate resistance of cemented clay. *J. Mater. Civ. Eng.* **29**, 4017160 (2017)
35. Cordon, W.A.: Resistance of soil-cement exposed to sulfates. 40th Annual Meeting of the Highway Research Board. Washington DC, USA (1962)
36. Attiogbe, E.K.; Rizkalla, S.H.: Response of concrete to sulfuric acid attack. *ACI Mater. J.* **85**, 481–488 (1988)
37. Chang, J.J.; Yeih, W.; Hung, C.C.: Effects of gypsum and phosphoric acid on the properties of sodium silicate-based alkali-activated slag pastes. *Cem. Concr. Compos.* **27**, 85–91 (2005)
38. Embong, R.; Kusbiantoro, A.: Study on the early hydration of cement paste containing sodium chloride. *Appl. Mech. Mater.* **621**, 35–38 (2014). <https://doi.org/10.4028/www.scientific.net/AMM.621.35>
39. Kalipcilar, I.; Mardani-Aghabaglou, A.; Sezer, G.I.; Altun, S.; Sezer, A.: Assessment of the effect of sulfate attack on cement stabilized montmorillonite. *Geomech. Eng.* **10**, 807–826 (2016)
40. Chegenizadeh, A.; Keramatikerman, M.; Miceli, S.; Nikraz, H.; Sabbar, A.S.: Investigation on recycled sawdust in controlling sulphate attack in cemented clay. *Appl. Sci.* **10**, 1–22 (2020). <https://doi.org/10.3390/app10041441>
41. Solanki, P.; Khoury, N.N.; Zaman, M.M.; et al.: Engineering properties of stabilized subgrade soils for implementation of the AASHTO 2002 pavement design guide. Final Report - Fhwa-Ok-08-10 Odot Spr Item Number 2185, School of Civil Engineering and Environmental Science, University of Oklahoma (2009)
42. Ghavami, S.; Jahanbakhsh, H.; Saedi Azizkandi, A.; Moghadas Nejad, F.: Influence of sodium chloride on cement kiln dust-treated clayey soil: strength properties, cost analysis, and environmental impact. *Environ. Dev. Sustain.* **23**, 683–702 (2021). <https://doi.org/10.1007/s10668-020-00603-6>
43. Pavlik, V.: Corrosion of hardened cement paste by acetic and nitric acids part II: formation and chemical composition of the corrosion products layer. *Cem. Concr. Res.* **24**, 1495–1508 (1994)

